2026 SCEC Annual Report

Calibration of the Near-Surface Seismic Structure in the San Francisco Community Velocity Model (SFCVM)

Report for SCEC Award 25291

PI: Dr. Kim B. Olsen

Institution: Department of Geological Sciences, San Diego State University, San Diego, CA 92182-1020

Publications and Reports:

Patel, A., and K.B. Olsen (2026). Calibration of the Near-surface Seismic Structure in the San Francisco Community Velocity Model (SFCVM), *Seism. Res. Lett.*, **97, 2B**, 1437-1438.

Summary

We have calibrated the near-surface structure of the San Francisco Community Velocity Model (SFCVM) with the aim to improve its ground motion prediction efficacy using Fourier Amplitude Spectral (FAS) bias up to 1 Hz via 3D physics-based wave propagation simulations for a series of M_w3.8–4.5 earthquakes. In areas of systematic underprediction we implement a V_{s30}-constrained spatially varying low-velocity taper (LVT), with the optimal station-specific thickness determined from trial-and-error simulations for different taper depths. The optimal spatially variable LVT reduces the FAS bias for areas outside the basins (defined as sites with surface Vs > 1 km/s) by up to 18% on average for the small earthquakes. In the San Francisco East Bay area, the addition of a shallow (25 - 75 m) low-velocity layer (Vs = 250 m/s) further improves the FAS bias by increasing the amplitudes and duration of the synthetics. In areas where the reference model systematically overpredicts amplitudes of the source ensemble, we calibrate the model by removing the near surface (up to 900 m) decrease in velocities, which further improves the FAS bias. The depth to the isosurface of Vs = 1.0 km/s ($Z_{1.0}$) in the SFCVM is increased by up to about 100 m outside the basins due to the implementation of the optimized LVT, with implications for the depth-dependent basin amplification terms used in Ground Motion Models.

Numerical Method and Data Processing

We performed 0–1 Hz 3-D wave propagation simulations using the GPU-supported staggered-grid finite-difference code AWP-ODC with a curvilinear discontinuous mesh (Cui et al., 2013, Nie et al., 2017, O'Reilly et al. 2021) in a rectangular model domain (see **Fig 1**). The spatial grid spacings were set to 50 m (top block) and 150 m (bottom block) with the grid partitions above and below 7.9 km and the model domain extending to a depth of 97 km. The minimum V_s included in the simulation is 250 m/s, ensuring a resolution of at least 5 points per minimum S-wavelength up to 1 Hz. Anelastic attenuation was incorporated via the linear velocity-dependent relation $Q_s = 0.1V_s$ and $Q_p = 2Q_s$.

For the validation, we processed strong motion recordings from the Northern California Earthquake Data Center (NCEDC) and corresponding synthetic time-series by applying a low-pass filter (10 Hz corner frequency), interpolating to a uniform time step, tapering the final 2 seconds, and padding with zeros for another 2 seconds. The horizontal components were rotated to E–W and N–S directions. The FAS of the velocities were subsequently calculated after applying a 0.2–1 Hz bandpass fourth-order Butterworth filter to avoid noise interference. We use Konno-Ohmachi smoothing (Konno and Ohmachi, 1998) with a bandwidth of 40 to suppress large fluctuations in the FAS.

Source Description of Validation Events

Ten moderate earthquakes (M_w3.8–4.5) were modeled using point-source descriptions. The moment-rate time history was described by a Brune-type minimum-phase function, expressed as

$$M(t) = M_0 \frac{t}{T^2 c} \exp\left(\frac{t}{Tc}\right),$$

where the characteristic time *Tc* controls the corner frequency, and the corner frequency is computed based on the local V_s and the stress drop (Madariaga, 1976). A global average stress drop of 3 MPa was used for all 10 validation events.

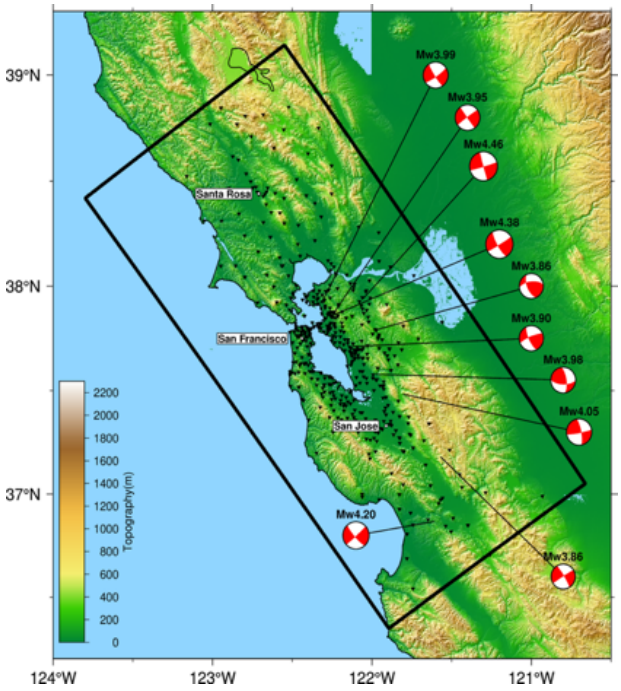

Figure 1. (left) Model domain (rectangle). Shading depicts surface topography. Beach balls show the focal mechanisms and epicenters of the 10 validation events. Black triangles show strong motion stations.

Estimation of Optimal LVT

To estimate the spatially variable LVT depth, we adopt a site-specific grid search optimization using the formulation of Ely et al. (2010). We conducted a suite of 0-1 Hz 3-D numerical simulations for the ensemble of earthquakes across fourteen discrete, constant taper depths (z_T) values constrained by V_{s30} data from Thompson et al. (2018). These transition depths range from 0 m (unmodified reference model), 90 m, 150 m, 200 m, 250 m, 300 m, 450 m, 600 m, 750 m, 900 m, 1200 m, 1500 m, 1800 m, and 2100 m). By simulating all events for each constant taper we obtain and evaluate the independent seismic response at each site as function of tapering depth.

The optimal z_T at each site is then determined by minimizing the empirical misfit between the simulated and recorded ground motions. We calculate the absolute three-component FAS and cumulative absolute velocity (CAV) bias, bandpass filtered between 0.2-1.0 Hz, for every site and event. At each site, the optimal taper depth is explicitly defined as the specific z_T value that yields the lowest absolute event-averaged FAS and CAV bias. These optimal site measurements are then spatially interpolated to generate a continuous 2-D map of optimal tapering depths across the entire computational domain.

To ensure that these structural modifications are physically justified and do not arbitrarily overwrite properly constrained basin features, the optimal LVT depth at each site is subject to additional statistical validation. Here, we employ a two-sample t-test to evaluate whether the bias for the estimated optimal LVT model is significantly smaller than that of the unmodified reference model at a 95% confidence level. This statistical check is activated for basin sites (surface Vs < 1000 m/s, generally considered reasonably well constrained) and any site where the grid search suggests an unexpected deep taper (z_T > 1200 m). If the test fails to reject the null hypothesis, the proposed LVT modification is discarded, and the localized structure reverts to the reference velocity model.

Results and Discussion

Simulations of the suite of small earthquakes using the reference model showed widespread underprediction of the recorded ground motions, particularly at rock sites. For example, simulations of the M_w4.38 Berkeley event severely underestimated the peak amplitude, FAS and the coda duration (see **Fig. 2,** 'SFCVM only'). Implementing a constant LVT with a taper depth of 600 m slightly improves the fit (7%). This widespread spatial underprediction (**Fig. 3**, **left**, LVT = 0 m) confirms that the reference SFCVM inherently features artificially stiff near-surface velocities, necessitating regional structural calibration.

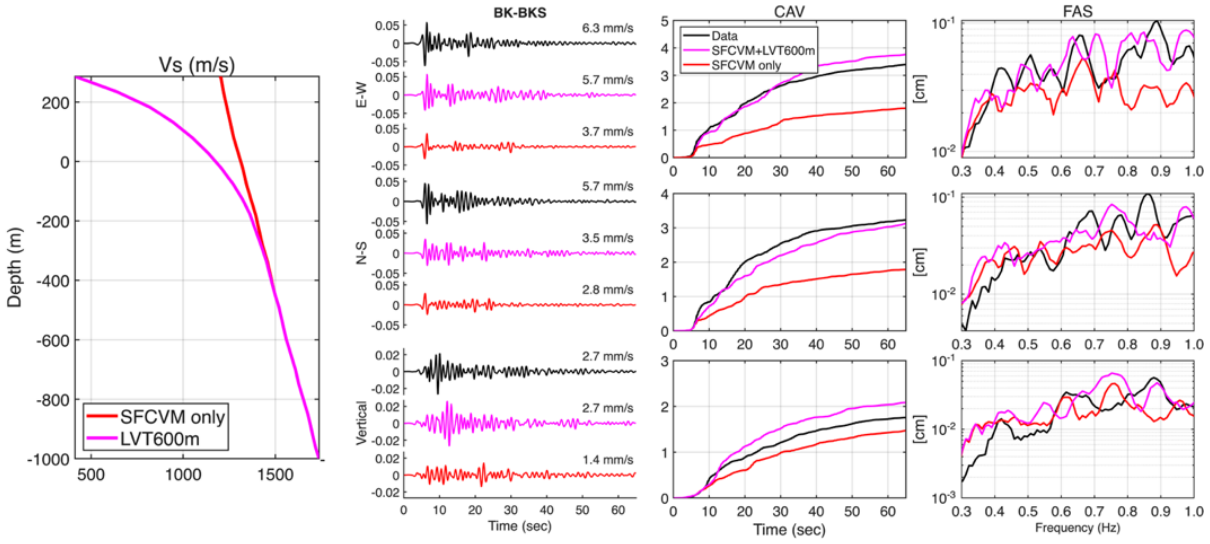

Figure 2. Illustration of the LVT (left) and the effects on ground motions at station BK-BKS (right) for LVT=600m tapering depth for the 2018/01/04 M_w4.38 event.

Figure 3, right shows the spatial distribution of LVT depths obtained from our optimization method, which includes depths from 0 to 2,100 m. Despite the improvement in fit to the recordings, localized areas of underprediction persist even for tapering depths of 2,100 m. The average optimal tapering depth across the entire domain is 467 m, increasing to 658 m specifically for Type B rock sites (surface Vs > 1000 m/s).

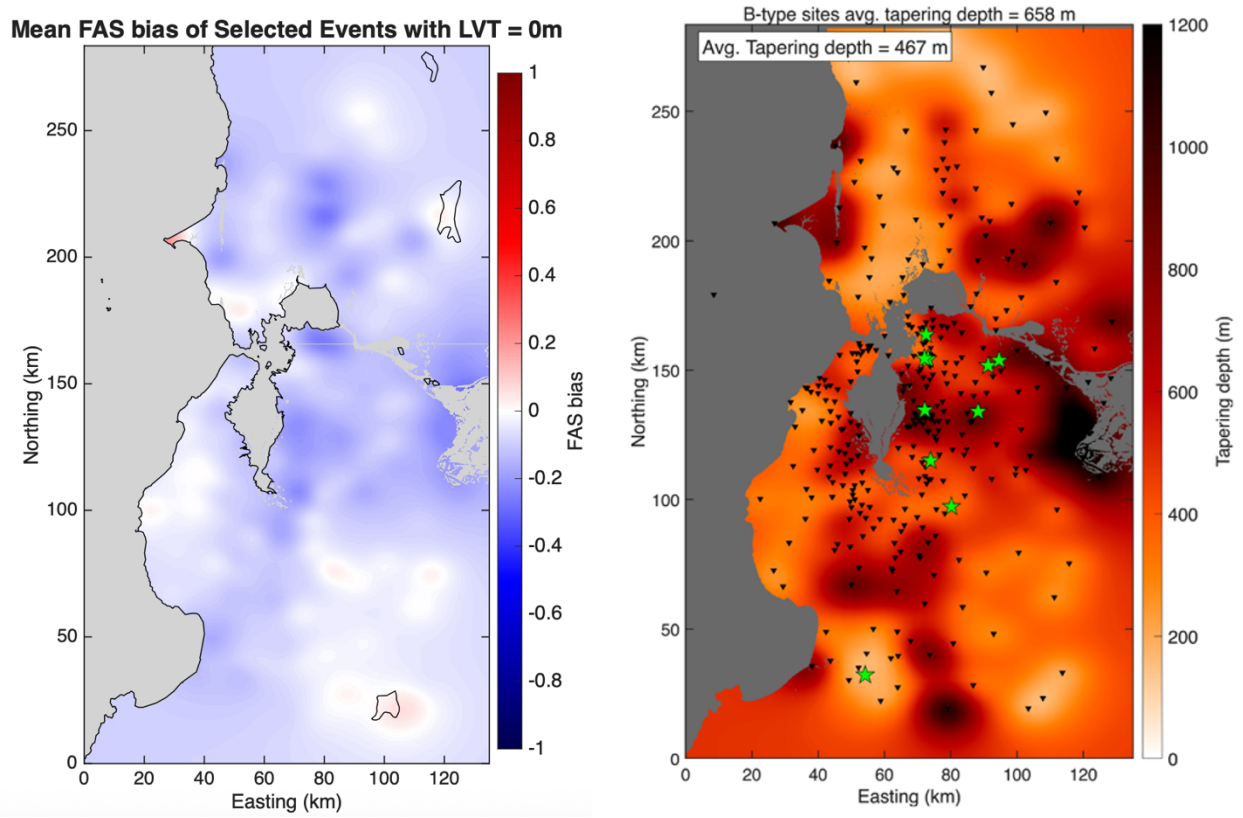

Figure 3. (left) Average FAS for all events with no LVT included. (right) Optimal, spatially interpolated optimal LVT depths. Triangles depict stations, stars show epicenters for validation events.

While the spatially variable LVT effectively resolved widespread underprediction, a subset of stations generate overprediction across the validation ensemble, even in the untapered (z_T = 0 m) reference model (see **Fig. 3, left**). This excessive amplification likely indicates that the native SFCVM assigns near-surface velocities with too low V_s. To correct this, we implemented a 'High Velocity Extension' (HVE) correction at these specific sites. By removing the near-surface velocity gradient and instead extending the deeper, high-velocity bedrock profiles and densities directly to the free surface (from depths of 900 m), we were able to decrease the amplification at many of the sites in question (e.g., HGS, see **Fig. 4**).

However, the spatially variable LVT failed to correct the underprediction at many sites in the East Bay. To further examine the reasons for the underprediction in the East Bay, we tested the effects of a shallow low-velocity layer (LVL) of Vs of 25-75 m thickness, capped at a minimum Vs of 250 m/s. The impedance contrast imposed by the LVL successfully trapped upward-propagating shear energy, increasing the duration of the synthetics and further reducing the residual underprediction in the East Bay (e.g., see CE58424, **Fig. 5**).

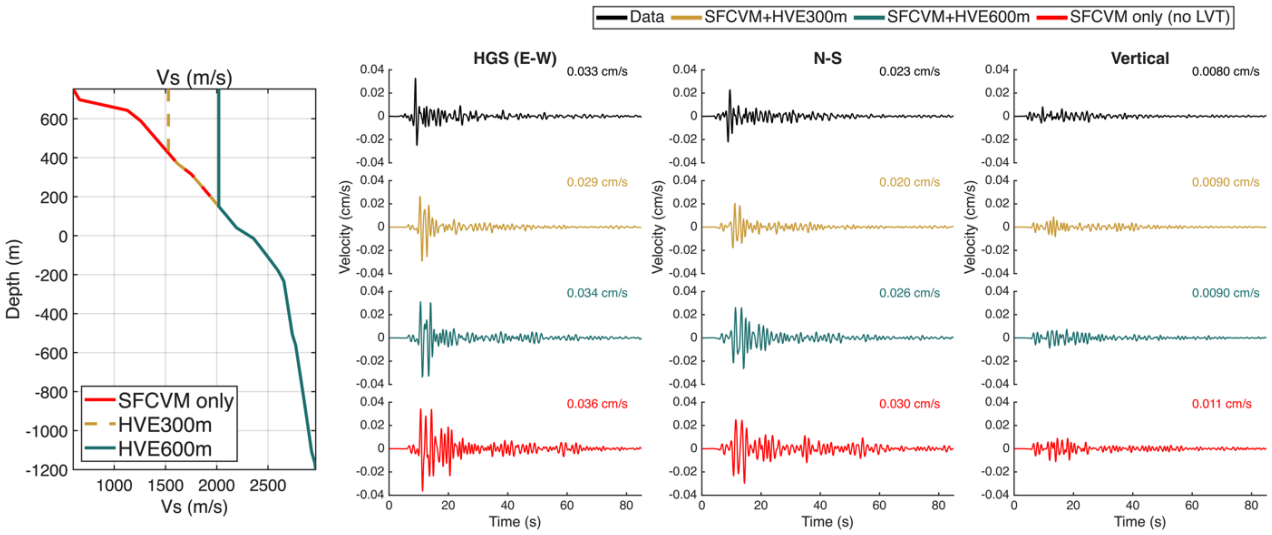

Figure 4. Illustration of the HVE (left) and the effects on the resulting ground motions at station HGS (right) for HVE300m and HVE600m for the 2018/01/04 M_w4.38 event.

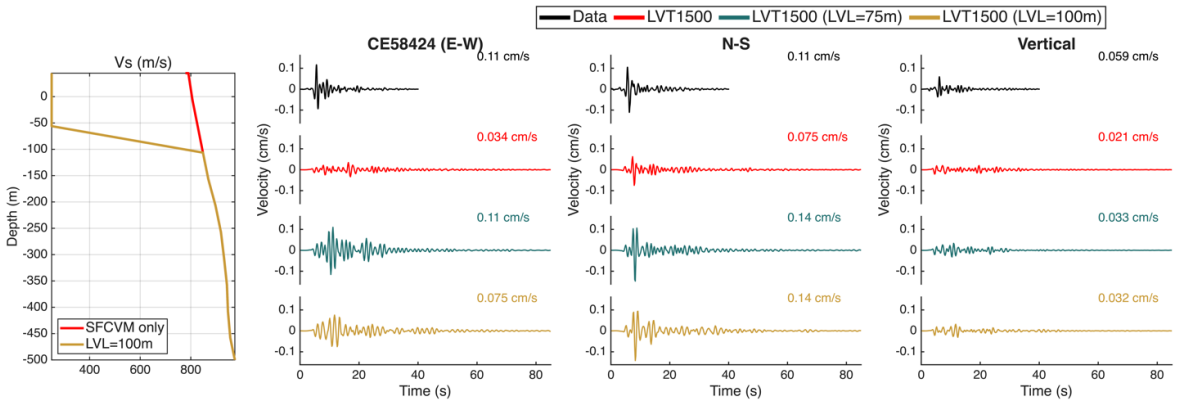

Figure 5. Illustration of the LVL (left) and the effects on ground motions at station CE58424 (right) for LVL=75m and LVL=100m for the 2018/01/04 M_w4.38 event.

Conclusions

We have calibrated the shallow crustal structure in the San Francisco Community Velocity Model (SFCVM) by validation of physics-based simulations and recorded ground motions for a suite of 10 small local earthquakes. The calibration resulted in a spatially-variable V_{s30}-constrained LVT, with depths varying between 0 and 2,100 m. We further reduced underpredictions of ground-motion bias in the East Bay by adding a discrete, shallow low-velocity layer, trapping high-frequency seismic energy. At other regions, we extended deeper, high-velocity bedrock profiles directly to the surface to reduce overprediction across our validation ensemble. The calibrated SFCVM establishes a basis for improved seismic hazard assessments in Northern California.

References

Aagaard, B.T., and Hirakawa, E.T., 2021, San Francisco Bay region 3D seismic velocity model v21.0: U.S. Geological Survey data release, https://doi.org/10.5066/P98CA3D5.

Brune, J. N., 1970, Tectonic stress and the spectra of seismic shear waves from earthquakes, J. Geophys. Res. 1896-1977, 75, no. 26, 4997–5009, doi: 10.1029/JB075i026p04997.

Cui, Y. et al., 2013, Physics-based seismic hazard analysis on petascale heterogeneous supercomputers, 1–12.

Ely, G. P., T. Jordan, P. Small, and P. J. Maechling, 2010, A VS30-derived nearsurface seismic velocity model, American Geophysical Union, Fall Meeting 2010, San Francisco, CA.

Hu, Z., K. B. Olsen, and S. M. Day, 2022a, 0–5 Hz deterministic 3-D ground motion simulations for the 2014 La Habra, California, Earthquake, Geophys. J. Int. 230, no. 3, 2162–2182, doi: 10.1093/gji/ggac174.

Hu, Z., K. B. Olsen, and S. M. Day, 2022b, Calibration of the near-surface seismic structure in the SCEC community velocity model version 4, Geophys. J. Int. 230, no. 3, 2183–2198, doi: 10.1093/gji/ggac175.

Konno, K., and T. Ohmachi, 1998, Ground-motion characteristics estimated from spectral ratio between horizontal and vertical components of microtremor, Bull. Seismol. Soc. Am. 88, no. 1, 228–241, doi: 10.1785/BSSA0880010228.

Madariaga, R., 1976, Dynamics of an expanding circular fault, Bull. Seismol. Soc. Am., 66, no. 3, 639–666.

Nie, S., Y. Wang, K. B. Olsen, and S. M. Day, 2017, Fourth-Order Staggered-Grid Finite-Difference Seismic Wavefield Estimation Using a Discontinuous Mesh Interface (WEDMI)Fourth-Order Staggered-Grid Finite-Difference Seismic WEDMI, Bull. Seismol. Soc. Am. 107, no. 5, 2183–2193, doi: 10.1785/0120170077.

O'Reilly, O., T. Yeh, K. B. Olsen, Z. Hu, A. Breuer, D. Roten, and C. A. Goulet, 2021, A High-Order Finite-Difference Method on Staggered Curvilinear Grids for Seismic Wave Propagation Applications with Topography, Bull. Seismol. Soc. Am. 112, no. 1, 3–22, doi: 10.1785/0120210096.

Pinilla-Ramos, C., Pitarka, A., M. EERI, D. M., and Nakata, R. (2025). Performance evaluation of the USGS velocity model for the San Francisco Bay Area. Earthquake Spectra. https://doi.org/10.1177/87552930241270575

Thompson, E. M., 2018, An Updated Vs30 Map for California with Geologic and Topographic Constraints, US Geol. Surv. Data Release, doi: 10.5066/F7JQ108S.